Author(s): Lipiäinen, Lauri & Jaakkola, Antti & Kokkonen, Kimmo & Kaivola, Matti

Title: Nonlinear excitation of a rotational mode in a piezoelectrically excited square-extensional mode resonator

Year: 2012

Version: Final published version

**Please cite the original version:**

Lipiäinen, Lauri & Jaakkola, Antti & Kokkonen, Kimmo & Kaivola, Matti. 2012. Nonlinear excitation of a rotational mode in a piezoelectrically excited square-extensional mode resonator. Applied Physics Letters. Volume 100, Issue 15. 153508. ISSN 1077-3118 (electronic). ISSN 0003-6951 (printed). DOI: 10.1063/1.3703119.

# Nonlinear excitation of a rotational mode in a piezoelectrically excited square-extensional mode resonator

Lauri Lipiäinen, Antti Jaakkola, Kimmo Kokkonen, and Matti Kaivola

Citation: Applied Physics Letters **100**, 153508 (2012); doi: 10.1063/1.3703119
View online: http://dx.doi.org/10.1063/1.3703119
View Table of Contents: http://scitation.aip.org/content/aip/journal/apl/100/15?ver=pdfcov
Published by the AIP Publishing

# Nonlinear excitation of a rotational mode in a piezoelectrically excited square-extensional mode resonator

Lauri Lipiäinen,[1] Antti Jaakkola,[2] Kimmo Kokkonen,[1] and Matti Kaivola[1]
[1]*Department of Applied Physics, Aalto University, P.O. Box 13500, 00076 Aalto, Finland*
[2]*VTT Technical Research Centre of Finland, Espoo, Finland*

(Received 18 January 2012; accepted 24 March 2012; published online 12 April 2012)

We present an experimental study of the nonlinear behavior of a square-extensional (SE) mode microelectromechanical resonator, actuated with a piezoelectric AlN thin film. The acoustic vibration fields of the device are characterized using laser probing. A nonlinear vibration behavior of the SE mode is observed above a drive power level of −10 dBm such that the vibration amplitude of the SE mode saturates and a rotational in-plane vibration mode is excited at a significantly lower frequency (0.725 MHz) than the SE mode (16.670 MHz). Interestingly, the measured ∼10 nm saturation amplitude of the SE mode is more than a decade below the amplitude value at which mechanical or electromechanical nonlinearities are estimated to become significant.
 [http://dx.doi.org/10.1063/1.3703119]

Microelectromechanical system (MEMS) silicon resonators are considered as potential alternatives to quartz crystals in timing and frequency control applications. Compared to quartz crystals that have dominated these markets over decades, the foreseen benefits of MEMS resonators include low cost, small size, low power consumption, and integrability with CMOS processing.[1] Piezoelectric thin-film actuation is a promising transduction method for MEMS silicon resonators.[2,3] While the more commonly used capacitive transduction provides resonances with a higher quality factor, even as high as $Q \sim 100000$ in the 10–100 MHz range[4,5] and $Q \sim 10000$ in the GHz range,[6] piezoelectric thin-film excitation can offer a better electromechanical coupling and, moreover, no DC bias or sub-100 nm gap structures are required as in capacitive coupling.

Compared to quartz crystals, the desirable smaller size of MEMS resonators unavoidably results in poorer energy storage, making it challenging to achieve an adequate phase noise performance.[7] Hence, the MEMS resonator should provide a vibration amplitude as high as possible for the best performance. In capacitively actuated Si resonators, the power handling capacity in linear operation is limited by both the nonlinear nature of the transduction method and the mechanical structure of the resonator.[7] The nonlinearity of the transduction is often the dominant one in capacitively driven resonators, but the effect can be reduced, e.g., by a more dedicated electrode configuration such as those used in comb-drive structures. The main mechanical nonlinearities are typically the nonlinearity of the resonator materials and the nonlinear geometrical effects caused by dynamic shape variations during vibration.

In the case of piezoelectric AlN thin-film-actuated MEMS Si resonators discussed here, the power handling capacity in linear operation is ultimately limited by the mechanical nonlinearities of the vibrating AlN-Si structure[8] and by the electromechanical nonlinearity of the AlN thin film. In a recent study,[9] the most dominant nonlinearity of AlN was shown to be the electromechanical nonlinearity, which, however, was observed to be nearly negligible at electric field strengths below 10 $\mathrm{V}/\mu\mathrm{m}$. In our experiments, the electric field strength was $< 1\mathrm{V}/\mu\mathrm{m}$, and hence, the nonlinearities of the AlN layer are expected to be small compared to the mechanical nonlinearities of the Si resonator structure.

The mechanical nonlinearities (and transduction nonlinearities in capacitive resonators) cause vibration amplitude dependent changes to the center frequency of the resonance, so-called spring-softening or spring-hardening effects (a.k.a. duffing effect). Increasing the vibration amplitude either decreases (spring softening) or increases (hardening) the center frequency of the resonance, and eventually, above a critical vibration amplitude $A_c$, the amplitude-frequency curve shows hysteresis (bifurcation). Although there have been some ideas of taking advantage of the bifurcation effect,[10–12] this effect is usually considered detrimental to resonators designed for linear operation, which in practice limits their power handling capacity.

In this letter, we have experimentally studied the acoustic behavior of a piezoelectrically driven square-extensional (SE) mode MEMS silicon resonator as a function of the input power. The in-plane (IP) and out-of-plane (OP) acoustic vibration fields of the device are characterized using optical probing. It is observed that when linearly increasing the drive power, the vibration amplitude of the 16.670-MHz SE mode first linearly increases and then, above a drive power level of $P_{\mathrm{TH}} = -10$ dBm, saturates to a nearly constant value. The corresponding saturation amplitude of the IP vibration is measured to be approximately 10 nm, which is more than an order of magnitude below the anticipated critical amplitude of bifurcation resulting from the mechanical nonlinearities of the resonator structure. Furthermore, the results show that, by driving the SE mode into the nonlinear regime where its vibration amplitude is saturated, a very pure rotational IP vibration mode is excited at 0.725 MHz, corresponding to the 23rd subharmonic frequency of the SE mode.

The structure of the square-plate resonator is illustrated in Fig. 1(a). The resonator is designed to operate in the SE mode at 16.670 MHz. The electrically measured quality factor for the SE mode operation (in vacuum, $< 1$ mBar) is $Q = 18\,000$ and the motional resistance is $R = 80\,\Omega$. The electrical characterization method is described in Ref. 13.

 

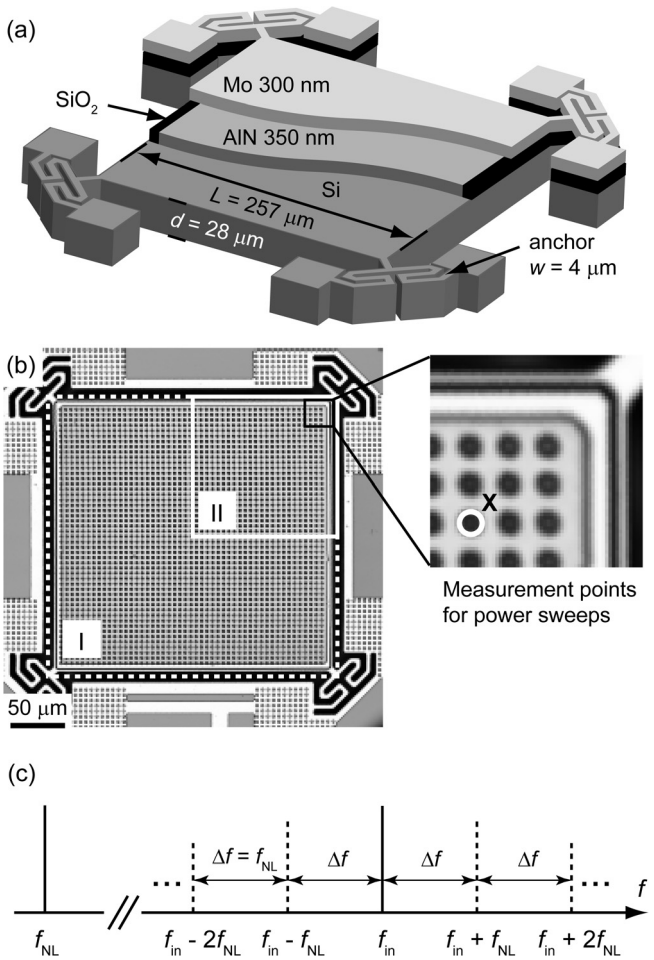


FIG. 1. (a) Schematic view of the sample. The 257 $\mu$m × 257 $\mu$m × 28 $\mu$m, single-crystalline Si resonator plate is piezoelectrically actuated with an AlN thin film. The Mo layer on top of the AlN layer acts as the top electrode, and the Si plate itself is used as the bottom electrode. The resonator is attached to the substrate at its corners with 4-$\mu$m-wide, meander anchors. (b) A microscope image of the resonator and illustration of the measurement areas used for optical characterization of the vibration fields. The top-electrode Mo layer is patterned with a 5-$\mu$m-period grid of circular, 2.5-$\mu$m-diameter holes in order to create reflectivity variations for IP detection. (c) Schematic representation of the frequency spectrum of the measurement signal, including signal artifacts caused by the nonlinearity of the optical detection (dashed lines) and the signals from the real acoustic modes (solid lines). The resonator is driven at $f_{in}$, resulting in the excitation of one vibration mode at $f_{in}$ and another at $f_{NL}$.

The acoustic vibration fields were measured using a scanning homodyne Michelson interferometer,[14] which is capable of amplitude and phase measurements of IP (Refs. 15 and 16) and OP (Ref. 17) surface vibration fields. The setup enables the use of different excitation and detection frequencies for studies of nonlinear acoustic phenomena.

The measurement areas in the sample geometry are depicted in Fig. 1(b). First, the amplitude of the IP and OP vibrations were measured at a single point as a function of the drive power of the single-frequency excitation. Care was taken to choose the measurement position in such a way that all relevant acoustic modes were detected. The OP measurement point, marked with "X" in Fig. 1(b), is located on the metal surface between the holes at the top-right corner of the resonator plate. The IP measurement point is at the right-hand side edge of the hole depicted with a white circle in Fig. 1(b). For each IP vibration mode, only the most sensitive point at the edge of the hole, i.e., the point where the normal of the edge is collinear with the direction of the vibration, is selected as the IP detection point. Areal measurements were then carried out on the resonator plate at selected excitation and detection frequency combinations in which the nonlinear acoustic behavior was observed. The OP measurement area I (267 $\mu$m × 267 $\mu$m) covers the whole resonator plate with a scan step of 1.54 $\mu$m. Due to the symmetry of the IP modes obtained in this study, the IP vibration field was measured only at the top-right quarter of the plate (scan area II: 134 $\mu$m × 134 $\mu$m, scan step 0.44 $\mu$m). The measurements were carried out in a low pressure environment (< 0.2 mBar) at room temperature.

It should be noted that the laser interferometric OP and the vectorial IP detection methods are themselves nonlinear in nature. Consequently, all the acoustic modes which simultaneously exist in the sample at different resonance frequencies are mixed in the detection, leading to artifacts in the detected signal. A schematic spectrum of such a measurement signal is depicted in Fig. 1(c) for the case of a MEMS resonator that features one mode at the input drive frequency $f_{in}$ and one nonlinearly excited mode at $f_{NL} \ll f_{in}$. In our experiments, we utilize the IP data of the areal measurements to identify the true acoustic modes based on the fact that, contrary to the laser interferometric OP data, the artifacts result in a different spatial content in the IP data than the real acoustic fields.

In the sample resonator, a nonlinear acoustic behavior was observed which was similar to the illustrative case of Fig. 1(c). When driving the sample at the SE mode excitation frequency of $f_{in} = f_{SE} = 16.670$ MHz above a threshold power of $P_{TH} = -10$ dBm, another mode gets nonlinearly excited at $f_R = 0.725$ MHz. The $f_R$ mode could not be electrically detected with this electrode geometry, but it was readily observed with the optical detection.

The detected IP vibration amplitudes of the two modes are presented in Fig. 2(a) as a function of the input drive power $P_{in}$, when the sample is driven at $f_{SE} = 16.670$ MHz. The nominal drive power $P_{in}$ is swept in the range from −41 to −6 dBm with 0.5 dBm steps. The mode at $f_R$ abruptly emerges at $P_{TH} = -10$ dBm. Above $P_{TH}$, the IP amplitude of the SE mode saturates, whereas the IP amplitude of the $f_R$ mode starts to increase with a slope approaching unity at $P_{in} > -9$ dBm. This indicates that above $P_{in} = -9$ dBm all the added power goes to the $f_R$ mode. Importantly, it should be noted that the $f_R$ mode cannot be directly excited via piezoelectric actuation at $f_R$ in this electrode geometry. Hence, the $f_R$ mode is a result of a truly nonlinear effect, emerging only by actuating the resonator at $f_{SE}$ with $P_{in} > P_{TH}$.

The IP vibration amplitudes of the SE and $f_R$ modes are illustrated in Fig. 2(b) as a function of the drive frequency, using three different drive power levels in the nonlinear regime ($P_{in} > P_{TH}$) and one in the linear regime. The drive frequency is swept both into increasing ($f_{in-up}$ sweep) and decreasing frequency ($f_{in-down}$ sweep) with 100 Hz frequency steps. In the nonlinear regime, the SE mode data clearly show the amplitude cutoff effect. However, the behavior is different for the $f_{in-up}$ and $f_{in-down}$ sweeps. For the up sweeps, the resonances extend higher in frequency, until, at certain drive frequencies depending on the power level, the

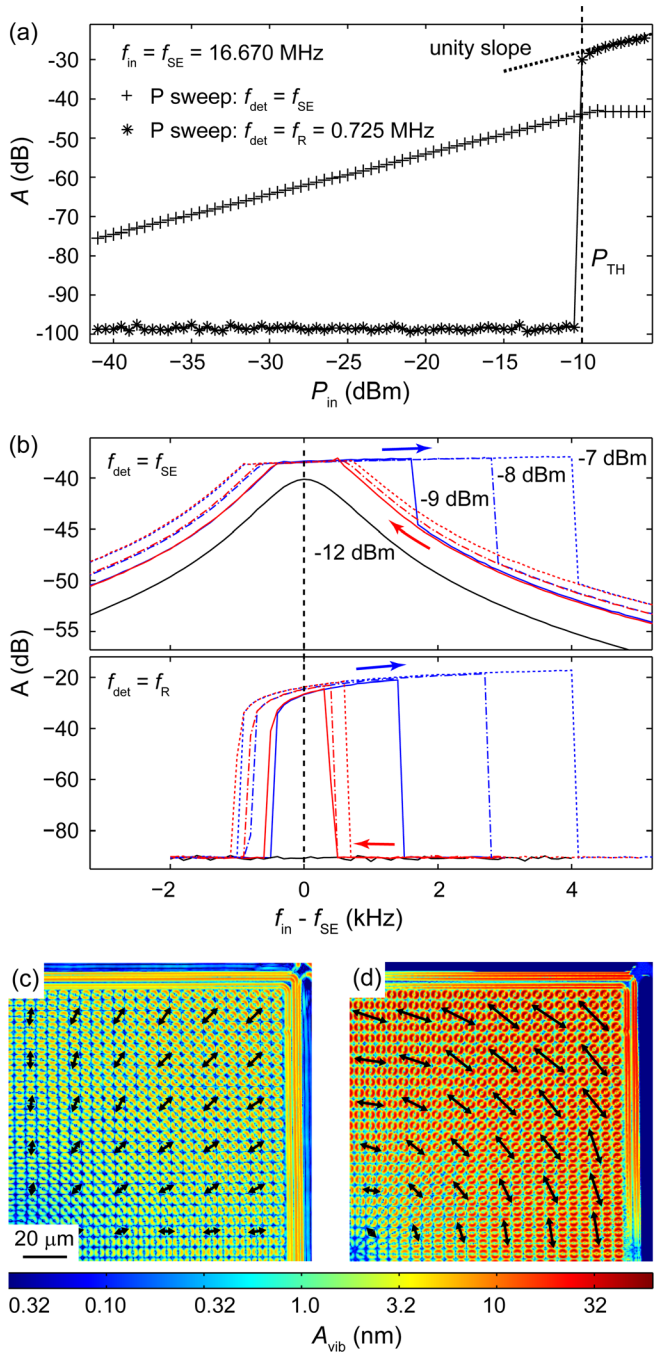


FIG. 2. (a) Measured relative IP vibration amplitude $A$ at $f_{SE} = 16.670$ MHz ("+") and at $f_R = 0.725$ MHz ("∗") as a function of the input drive power ($f_{in} = f_{SE} = 16.670$ MHz). (b) The relative IP vibration amplitude detected at $f_{SE}$ (top) and at $f_R$ (bottom) as a function of $f_{in}$, using four different $P_{in}$ levels (−12 dBm solid black line, −9 dBm solid, −8 dBm dashdotted, and −7 dBm dotted blue/red line). In the nonlinear regime, $P_{in} > -10$ dBm, the drive frequency $f_{in}$ is swept both upward (blue lines) and downward (red) in frequency. (c) IP vibration amplitude $A_{vib}$ and vector fields of the $f_{SE} = 16.670$ MHz and the (d) $f_R = 0.725$ MHz mode, when the sample is driven with $P_{in} = -8$ dBm at $f_{in} = 16.670$ MHz.

amplitude abruptly drops down. No such asymmetric broadening of the resonance is observed for the down sweeps. Similar broadening behavior for the $f_{in-up}$ sweeps is observed also for the $f_R$ mode. In addition, the $f_{in-up}$ and $f_{in-down}$ sweeps of the $f_R$ mode show hysteresis effect which is characteristic for spring hardening.

The measured IP vibration fields of the $f_{SE}$ mode and the $f_R$ mode are illustrated in Figs. 2(c) and 2(d). In these areal scans, the resonator is driven in the nonlinear regime with $P_{in} = -8$ dBm at $f_{SE}$. Although the IP vibration amplitude of the SE mode is saturated to a maximum of ∼10 nm in this regime, its vibration field pattern is still characteristic to the SE mode, similar to the one obtained in the linear operation range, $P_{in} < P_{TH}$. Also the shape of the OP SE vibration field was found to stay unchanged in the nonlinear range, but the amplitude saturates.

The IP data of the $f_R$ mode correspond to an IP vibration mode with radially symmetric rotational vibration of the resonator plate with the corner anchors acting as springs. Interestingly, there is no detectable OP component, indicating the mode to be purely rotational. The measured maximum IP amplitude of this rotational mode is even higher than that of the SE mode, see Figs. 2(c) and 2(d). It was also confirmed using FEM simulations that such a $f_R$ mode indeed can exist in this resonator structure at this frequency.

The nonlinearity observed in this study severely degrades the power handling capacity of the resonator sample. The obtained IP saturation amplitude for the SE mode is approximately 10 nm, whereas the bifurcation amplitude due to mechanical nonlinearities has been estimated to be > 300 nm in this resonator structure. This estimation is based on a limit obtained previously in a capacitive SE mode resonator with a similar Si resonator structure,[7] which is scaled to the dimensions and the $Q$ value of our resonator. Hence, the mechanical nonlinearity of the resonator structure does not explain the low nonlinearity limit obtained.

Avoort *et al.*[18] have reported a nonlinear behavior in capacitively actuated MEMS resonators, which shows similarities to the observations of our study, such as the amplitude saturation and the excitation of another acoustic mode at a different frequency than the excitation frequency. They proposed the nonlinear behavior to be related to an autoparametric resonance. However, we observe an amplitude-frequency hysteresis in our sample resonator, a feature not explained by the autoparametric resonance in a linear system. The 1:23 frequency ratio between the $f_R$ and $f_{SE}$ modes would indicate that they may be mechanically coupled, thus resulting in a nonlinear parametric excitation.[19] Dedicated simulations and further experiments in varying dimensions are needed to explain in detail the nonlinear effects observed.

A.J. acknowledges funding from the Academy of Finland.

[1]C. T.-C. Nguyen, IEEE Trans. Ultrason. Ferroelectr. Freq. Control. **54**, 251–270 (2007).
[2]R. Abdolvand, H. Lavasani, G. Ho, and F. Ayazi, IEEE Trans. Ultrason. Ferroelectr. Freq. Control **55**, 2596–2606 (2008).
[3]A. Jaakkola, P. Rosenberg, S. Asmala, A. Nurmela, T. Pensala, T. Riekkinen, J. Dekker, T. Mattila, A. Alastalo, O. Holmgren, and K. Kokkonen, in *Proceedings of the IEEE Ultrasonics Symposium*, Beijing, China, 2-5 November 2008 (IEEE, New York, 2008), pp. 717–720.
[4]V. Kaajakari, T. Mattila, A. Oja, J. Kiihamäki, and H. Seppä, IEEE Electron Device Lett. **25**, 173–175 (2004).
[5]N. D. Badilaf-Ciressan, M. Mazza, D. Grogg, and A. M. Ionescu, Solid-State Electron. **52**, 1394–1400 (2008).
[6]J. Wang, J. E. Butler, T. Feygelson, and C. T. C. Nguyen, in *Proceedings of the IEEE 17th International Conference on MEMS*, Maastricht, The Netherlands, 25–29 January 2004 (IEEE, New York, 2004), pp. 641–644.
[7]V. Kaajakari, T. Mattila, A. Oja, and H. Seppä, J. Microelectromech. Syst. **13**, 715–724 (2004).
[8]C. Zuo, N. Sinha, J. Van der Spiegel, and G. Piazza, J. Microelectromech. Syst. **19**, 623–627 (2010).

[9]W. Sahyoun, J.-M. Duchamp, and P. Benech, IEEE Trans. Ultrason. Ferroelectr. Freq. Control **58**, 2162–2170 (2011).
[10]M. Pardo, L. Sorenson, and F. Ayazi, in *Proceedings of the IEEE International Symposium on Circuits and Systems*, Rio de Janeiro, Brazil, 15-18 March 2011 (IEEE, New York, 2011), pp. 221–224.
[11]V. Kumar, J. W. Boley, Y. Yang, H. Ekowaluyo, J. K. Miller, G. T.-C. Chiu, and J. F. Rhoads, Appl. Phys. Lett. **98**, 153510 (2011).
[12]A. Hajati, S. P. Bathurst, H. J. Lee, and S. G. Kim, in *Proceedings of the IEEE 24th International Conference on MEMS 2011, Cancun, Mexico, 23-27 Jan 2011* (IEEE, New York, 2011), pp. 1301–1304.
[13]A. Jaakkola, J. Lamy, J. Dekker, T. Pensala, L. Lipiäinen, and K. Kokkonen, in *Proceedings of the IEEE International Frequency Control Symposium*, Newport Beach, California, USA, 1–4 June 2010 (IEEE, New York, 2010), pp. 410–414.
[14]J. V. Knuuttila, P. T. Tikka, and M. M. Salomaa, Opt. Lett. **25**, 613–615 (2000).
[15]O. Holmgren, K. Kokkonen, T. Mattila, V. Kaajakari, A. Oja, J. Kiihamäki, J. V. Knuuttila, and M. M. Salomaa, Electron. Lett. **41**, 16–17 (2005).
[16]O. Holmgren, K. Kokkonen, T. Veijola, T. Mattila, V. Kaajakari, A. Oja, J. V. Knuuttila, and M. Kaivola, J. Micromech. Microeng. **19**, 015028 (2009).
[17]L. Lipiäinen, K. Kokkonen, and M. Kaivola, J. Appl. Phys. **108**, 114510 (2010).
[18]C. van der Avoort, R. van der Hout, J. J. M. Bontemps, P. G. Steeneken, K. L. Phan, R. H. B. Fey, J. Hulshof, and J. T. M. van Beek, J. Micromech. Microeng. **20**, 105012 (2010).
[19]W. K. Tso and T. K. Caughey, J. Appl. Mech. **32**, 899–902 (1965).